*J. Electrochem. Sci. Eng.* **14(2)** (2024) 247-263; http://dx.doi.org/10.5599/jese.2228

Open Access : : ISSN 1847-9286
https://pub.iapchem.org/ojs/index.php/JESE

*Original scientific paper*

# The effect of coating drying conditions on bronze corrosion protection

Helena Otmačić Ćurković, Angela Kapitanović✉, Martina Filipović and Petra Gorišek

*University of Zagreb Faculty of Chemical Engineering and Technology, Research Laboratory for Corrosion Engineering and Surface Protection, Savska 16, HR 10000 Zagreb, Croatia*

*Corresponding author:* ✉akapitano@fkit.unizg.hr; *Tel.: +385-1-4597-126*

Received: December 22, 2023; Accepted: February 8, 2024; Published: February 12, 2024

***Abstract***

*Waterborne coatings present a green alternative to solvent-borne coatings as only a small amount of organic solvent is released into the environment during drying. However, for waterborne coatings, the drying process is much more challenging due to the slow evaporation of water. In this work, the influence of drying temperature on the protective properties of a waterborne acrylic coating was studied. Its performance in corrosion protection of bronze substrates, representing the bronzes used for the sculptures placed outdoors, was examined. Corrosion properties were evaluated by linear polarization measurements and electrochemical impedance spectroscopy during three-week exposure to artificial acid rain solution. It was found that drying at ambient temperature resulted in modest corrosion protection, while drying at 55 °C ensured greater initial corrosion resistance, which gradually degraded during exposure to acid rain solution accompanied by the coating blistering. Drying of one-layer coating at 40 °C resulted in the formation of clearly visible corrosion products. If the coating was applied in three layers, the drying process was more efficient, leading to slightly higher polarization resistance values without visible corrosion at the bronze surface. Furthermore, the studied waterborne acrylic coating provided good corrosion protection of patinated bronze surfaces. Additionally, it was found that for efficient corrosion protection, it is preferable that the coating contains a corrosion inhibitor in order to avoid substrate corrosion during coating drying. When applied properly, studied coating does not alter the state of surfaces, both bare and patinated, which is important for its application in bronze cultural heritage protection.*

**Keywords**

Waterborne coatings; drying temperature; electrochemical impedance spectroscopy; polarization measurements

## Introduction

Bronze cultural heritage placed outdoors is gradually covered with a natural patina due to the corrosion process. The formation of patina will take longer in less aggressive environments, but it will

proceed faster in polluted ones [1]. Bronze corrosion can result in the formation of both stable and unstable corrosion products. These unstable products can, in the presence of moisture and oxygen, cause further degradation and endangerment of works of art [2,3]. In order to prevent gradual surface deterioration, protective organic coatings are widely used [4].

Over the past few decades, new legislatives have altered the perspective on the effects of solvent-borne organic coatings on the environment and human health. For that reason, the coating industry has developed environmentally friendly waterborne coatings resulting in improved air quality and reduced hazard impact on the surroundings. Waterborne adhesives, paints and coatings are becoming of more interest because a high concentration of volatile organic compound (VOC) is replaced by water [5-7]. In addition, they contain anticorrosive pigments without heavy metals, resulting in a non-toxic and non-flammable solution [8-10].

Waterborne coatings drying occurs in three stages: 1) the solvent (water) evaporation, 2) the polymer nanoparticles deformation, where a densely packed structure is created, and 3) the polymer chains interdiffusion leading to coalescence [11,12]. The film particles will deform and achieve closer contact, forming a rigid film structure when the film is above the minimum film formation temperature [13,14]. The strength of the polymer interface is determined by the degree of entanglements between the polymer chains [15]. In addition, the rate of evaporation depends on the difference in vapour pressure between the water in the coating and the air being circulated over the substrate. A large amount of water in the coating results in a prolonged drying duration in cold and humid environments [16]. Slow coating drying means that if the coating is applied directly on the metal surface, there will be prolonged contact between the metal and the water, which can lead to substrate corrosion.

Hwang *et al.* [17] investigated how the morphology and surface characteristics of the waterborne UV-curable coatings were affected by the water drying conditions. After testing drying temperatures of 22, 50 and 80 °C and various drying durations, the researchers concluded that too low drying temperature led to surface cracking, peeling and blistering of a cured coating. The improvement of hardness and adhesion strength was noted at higher drying temperatures and rates.

Three drying temperatures (5, 23 and 35 °C) were examined by Stojanović *et al*. in the study on curing temperature influence on corrosion protection properties of waterborne and solventborne epoxy coatings [16]. For the solventborne coating, all tested drying temperatures resulted in a coating with stable, protective properties, whereas that was not the case for waterborne coating. When dried at 35 °C, it demonstrated the best level of corrosion resistance, while certain limitations were noted at lower testing temperatures. They concluded that elevated curing temperatures were needed to obtain higher performance of waterborne coatings, either in corrosion protection or physical properties. Also, raising the layer thickness had a beneficial impact, but only to a certain value, because it may result in prolonged drying time and insufficient water evaporation [16]. To achieve the optimum final qualities of a coating, in terms of application and surface morphology, adequate drying at the right temperature was found to be very important [16,17].

The aim of this work is to examine how drying temperature and a number of applied layers affect waterborne acrylic coatings' ability to protect bronze cultural heritage from corrosion. For cultural heritage protection, it is important that the coating does not alter the surface appearance, thus, for this study, two clear waterborne coatings were selected. One of these coatings is a commercial product (C2) and another is under development (C1). The main difference in these coatings is that C1 contains a corrosion inhibitor and less water. Our goal was not to study a particular coating or corrosion inhibitor but to examine the conditions under which waterborne acrylic coatings could be applied for protection of bronze cultural heritage. Drying waterborne coatings is quite challenging, as

too low temperature can lead to slow drying and substrate corrosion, while too high temperatures result in coating cracking. In addition, water in the coating can have different effects on bronzes of different compositions as well as on the patina that is usually present on bronze sculptures. Studies were conducted on different bronze substrates, typically found on objects of cultural heritage, to determine if the coating performance significantly depends on substrate properties. Besides bare bronzes, studies were also conducted on bronze surfaces covered by a layer of patina. Coating protection efficiency was examined using linear polarization measurements (LP) and electrochemical impedance spectroscopy (EIS) during the immersion in artificial acid rain.

## Experimental

### *Sample preparation*

In this study, three different kinds of bronzes were used: RG7, CuSn12 with 1.33 $cm^2$ of exposed surface and CuSn6 with 1.5 $cm^2$. All bronzes were obtained from Strojopromet Ltd., Croatia and their composition is presented in Table 1. In order to prepare working electrodes for electrochemical measurements, bronze discs, together with soldered copper wire, were embedded into an epoxy resin. Afterwards, the surface was polished with SiC papers (80, 800, 1200 and 2500), degreased in an ultrasonic ethanol bath and rinsed with deionized water. Part of the bronze samples was used for artificial patination, either chemically or electrochemically, as described in our previous work [18].

***Table 1.*** *The composition of tested bronzes*

| Sample | Content, wt.% | | | |
|---|---|---|---|---|
| | Cu | Sn | Zn | Pb |
| RG7 | 83.25 | 4.6 | 4.58 | 5.85 |
| CuSn12 | 87.94 | 11.02 | 0.07 | 0.54 |
| CuSn6 | 94.0 | 6.0 | - | - |

The investigation was conducted with two acrylic waterborne coatings named C1 and C2. Coating C1 is non-commercial and was obtained from the research department of one paint company, whereas C2 is a commercial product obtained from the same paint company. The main difference between these coatings is that C1 contains corrosion inhibitor and a slightly lower amount of water compared to C2. Both coatings were applied manually on bronze surfaces by brushing at room temperature.

RG7 bronze substrate served for the study of the influence of drying temperature and the number of layers of C1 coating on the corrosion protection properties. Three different drying temperatures (24, 55 and 40 °C) were tested. Examined experimental conditions are shown in Figure 1a. A comparative study between two waterborne coatings was performed on different bronze substrates: RG7, CuSn12 and CuSn6. For these studies, three layers of coatings were applied and dried at 40 °C, as presented in Figure 1b. Finally, various chemically or electrochemically patinated bronzes were also protected by waterborne coating C1 applied in three layers and dried at 40 °C (according to Figure 1b). Prior to further characterization, all samples were placed in a desiccator for 10 days.

The determination of dry film thickness on studied samples was conducted by PosiTector 600 (DeFelsko) and is presented in Table 2.

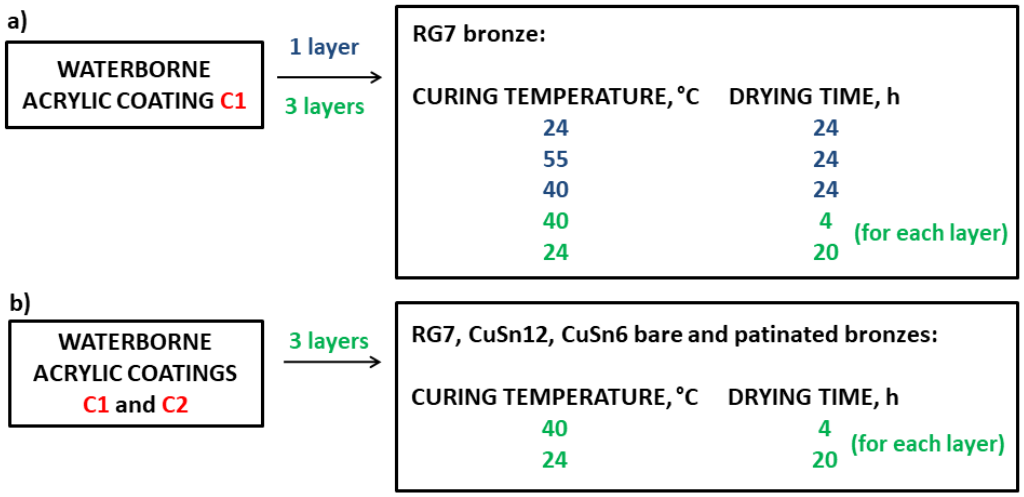


***Figure 1.*** *Experimental conditions for application of the coatings for study of: (a) drying temperature influence, (b) substrate composition influence*

***Table 2.*** *Thickness of coated samples for electrochemical measurements*

| | Sample | Thickness, µm |
|---|---|---|
| RG7 bronze covered with C1 for investigation of drying temperature and the number of layers | 1 layer, 24 °C | 35 ± 8 |
| | 1 layer, 55 °C | 30 ± 11 |
| | 1 layer, 40 °C | 62 ± 14 |
| | 3 layers, 40 °C | 27 ± 5 |
| Various bronzes protected with C1 or C2 coatings | C1/CuSn12 | 15 ± 2 |
| | C1/CuSn6 | 18 ± 8 |
| | C1/RG7 | 27 ± 5 |
| | C2/RG7 | 33 ± 6 |
| | C2/CuSn6 | 49 ± 2 |
| Sulphate patina protected with C1 coating | C1/CuSn12 | 11 ± 3 |
| | C1/CuSn6 | 14 ± 5 |
| | C1/RG7 | 13 ± 6 |
| Electrochemical patina protected with C1 coating | C1/CuSn12 | 18 ± 5 |
| | C1/CuSn6 | 16 ± 8 |

*Coating characterization*

The characterization of the protective properties of coatings was conducted by electrochemical measurements: linear polarization (LP) and electrochemical impedance spectroscopy (EIS). Measurements were carried out in simulated acid rain (0.2 g $l^{-1}$ $NaNO_3$ (*p.a.*), from T.T.T., Croatia, 0.2 g $l^{-1}$ $NaHCO_3$ (*p.a.*) and 0.2 g $l^{-1}$ $Na_2SO_4$ (*p.a.*) from Kemika, Croatia in redistilled water) with pH 5 (adjusted with 0.5 M $H_2SO_4$, at room temperature). All corrosion tests were carried out with a potentiostat Bio-Logic SP-300, France. A three-electrode cell arrangement was used. A coated bronze served as a working electrode, a saturated calomel electrode (SCE) as a reference and a graphite rod as a counter electrode. Electrochemical measurements were conducted after 45 minutes of open circuit potential ($E_{OCP}$) stabilization. LP was conducted in a narrow potential range (± 25 mV *vs*. $E_{OCP}$). EIS was performed at $E_{OCP}$ with an amplitude of 10 mV. The frequency range for EIS was 100 kHz to 10 mHz with 6 points per decade. The impedance analysis was conducted in ZSimpWin 3.60 software with data weighting factor 1.

In addition, gravimetric measurements were conducted in order to determine the percentage of mass increase during the coating soaking in acid rain solution. For this testing, both coatings (C1 and C2) were applied on aluminium foil and dried at 40 °C for 24 h. Each coating sample was weighed before and after drying using a Radwag AS 60/220.X2 Plus, analytical balance (Poland). After drying, samples were left to swell in the acid rain solution, from which they were periodically removed (after

8 and 126 h). The samples were weighed and immediately re-immersed in the solution. Excess water from the coating surface was removed with a gentle wiping by a towel.

## Results and discussion

*Effect of drying temperature and number of layers on the coating protective properties*

The waterborne acrylic coating C1 was applied on RG7 bronze electrodes and dried at different temperatures. The coating was dried either at ambient temperature (24 °C) or at elevated temperatures (55 and 40 °C). In addition, samples with three-layer coating were prepared and dried at 40°C. These samples were prepared so that coating was applied in three thin layers whose total thickness was similar to that of one-layer coating. The intention was to determine if better protection is obtained by coating application in several thin layers or one thicker layer. The protective properties of these coatings were examined by linear polarization measurements during the three-week immersion of bronze samples in artificial acid rain solution. From such obtained polarization curves, polarization resistance values were determined and shown in Figure 2. In general, obtained polarization resistance ($R_p$) values are almost two orders of magnitude lower than those observed for bronze covered by Paraloid B44, the most common acrylic solvent-based coating for the protection of bronze cultural heritage, examined under similar conditions [19].

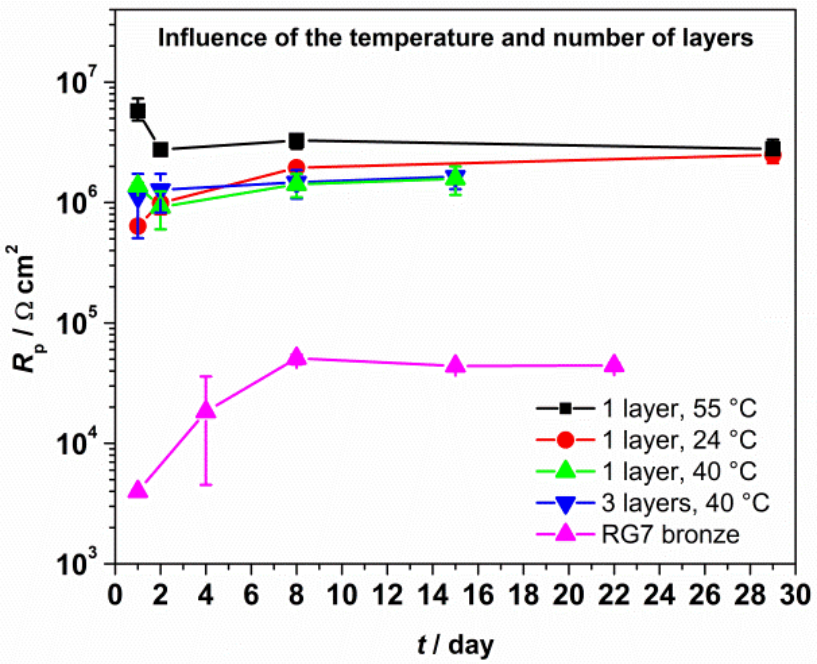


***Figure 2.*** *Dependence of polarization resistance on immersion time in acid rain solution for differently dried coatings*

However, it is common to see that solvent-based coatings have superior performance to waterborne coatings. Initial measurements showed that higher drying temperature resulted in initially higher coating $R_p$ values. On the other hand, initially, there was no significant difference between one- and three-layer coatings dried at the same temperature. However, with the prolonged immersion time an increase in $R_p$ value was observed for coating dried at 24 °C and less pronounced for three-layer coating at 40 °C. For coatings dried at 55 °C and for one-layer coatings at 40 °C, $R_p$ decreased on the second day of immersion, followed by a more or less exhibited increase in $R_p$ with a further immersion period. In order to better understand the observed variations in $R_p$ values, a more detailed analysis was carried out by means of electrochemical impedance spectroscopy.

EIS spectra obtained for bronze with coating cured at 24 °C are presented in Figure 3. The phase angle plot exhibited two maxima, already on the first day of immersion in acid rain solution. This is a clear indication of the presence of water in the coating and at the metal surface, as for the well-protective coatings with no water reaching the metal surface, only one wide phase angle maxima close to -90° would be observed [20-23]. It can be assumed that the coating was not fully dried, *i.e.,* the water remained in the coating and penetrated towards the metal surface. For the second day of immersion, an increase in impedance modulus values in the low-frequency region was observed. Finally, for the last day of immersion, an increase in the value of impedance modulus is visible at both high- and low-frequency regions. In addition, the width of the phase angle curve maximum at high frequencies increased compared to the second day. So, it appears that the protective properties of the coating have improved over time. In their study of different waterborne coatings dried at room temperature, Jianguo *et al.* [24] came to the conclusion that insoluble corrosion products accumulation in the pores of the coating leads to the closure of the pores and improved coating barrier properties. In our study, the presence of corrosion products below the clear coating was not visible to the naked eye (Figure 4a) but can be deduced from the shape of the EIS spectra. However, small bubbles were observed that formed during coating drying, which could lead to easier coating failure. A similar problem was observed by Hwang *et al*. [17] for coating dried at low temperatures.

EIS spectra were analysed by fitting the equivalent electrical circuit shown in Figure 5a to experimental data. The circuit includes three *R*-*Q* couples. Although only two phase angle maxima are clearly observed in the spectra shown in Figure 3, it was not possible to obtain a good fit of the spectra without using the model with three time constants. The electrolyte resistance in all measurements was around 500 Ω cm$^2$. The first *R*-*Q* couple is noted at the highest frequencies region and is related to the presence of corrosion products ($R_F$-faradaic resistance of electrochemical reaction involving corrosion products; $Q_F$-capacitance of corrosion products). *R*-*Q* pair related to the phase angle maxima in the medium to high-frequency region describes the properties of the coating ($R_{po}$ – resistance of the pores in the coating and $Q_f$-constant phase element representing the coating capacitance), while the medium to low-frequency region is related to the corrosion process on the metal surface ($R_{ct}$-charge transfer resistance and $Q_{dl}$-constant phase element representing a double-layer capacitance). The coefficients $n_F$, $n_f$ and $n_{dl}$ describe nonideal capacitive behaviour. A similar model was used by Collazo *et al*. [25] for the description of EIS spectra of a waterborne resin applied on a galvanized steel substrate. However, in their work, the time constant related to the presence of corrosion products was observed in the medium frequency region.

The obtained impedance parameters are presented in Table 3. The general principle applied in this work for validation of fitting quality was that chi-square value for all fitted spectra must be below $10^{-3}$, and that there are no more than one-half of parameters with relative standard error above 10 %. In this case, it can be observed that both $Q_F$ and $R_F$ values were increasing in time. This can be explained by the increase in the amount of corrosion products on the bronze surface. It should be stressed that for the first day, $R_F$-$Q_F$ values are not fully reliable as only a few points at the high-frequency region correspond to this couple. Regarding the second *R*-*Q* couple, an increase in $Q_f$ from the first to the second day of immersion is due to the penetration of water from the acid rain solution, as the water has a higher dielectric constant compared to organic coating. Such behaviour is often observed for organic coatings in contact with water [20,26,27]. However, on the 29$^{th}$ day of immersion, a decrease in coating capacitance is visible. Additionally, an increase in $R_{po}$ and $R_{ct}$ values is observed, as well as a decrease in $Q_{dl}$ values. Usually, the opposite behaviour is expected as the result of water penetration into the coating and an increase of metal surface area

in contact with water. The improvement of corrosion resistance in time, observed in this work, could be caused by the formation of corrosion products that were closing the pores of the coating and covering the metal surface in the bottom of the pores. Low $n_{dl}$ values obtained for the first day of immersion suggest the influence of diffusion, of species participating in corrosion reaction through the pores of the coating, on the overall corrosion rate.

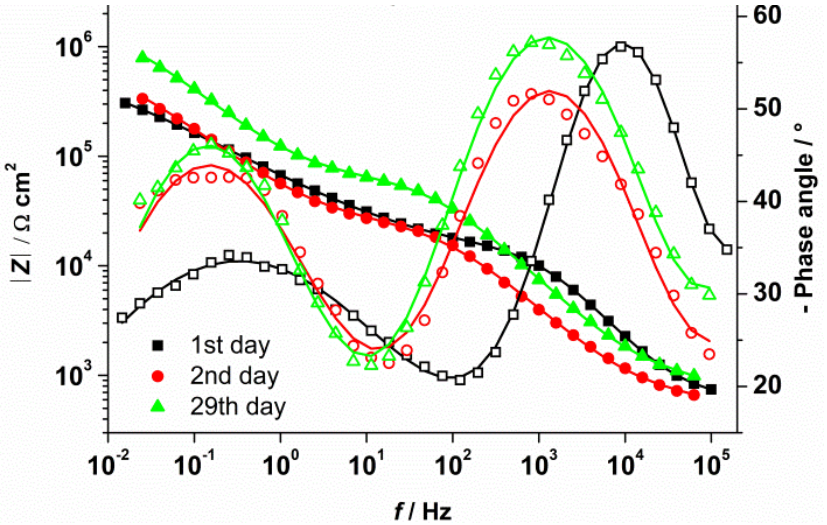


***Figure 3.*** *EIS spectra for one layer of coating dried at 24°C (solid symbols-impedance; open symbols-phase angle). Experimental data are depicted in symbols and fitted data in lines*


***Figure 4****. Surface image of RG7 bronze coated with one layer of waterborne acrylic coating C1 dried at: (a) 24 °C, (b) 55 °C and (c) 40 °C for 24 hours. Images were taken upon the immersion in acid rain solution*

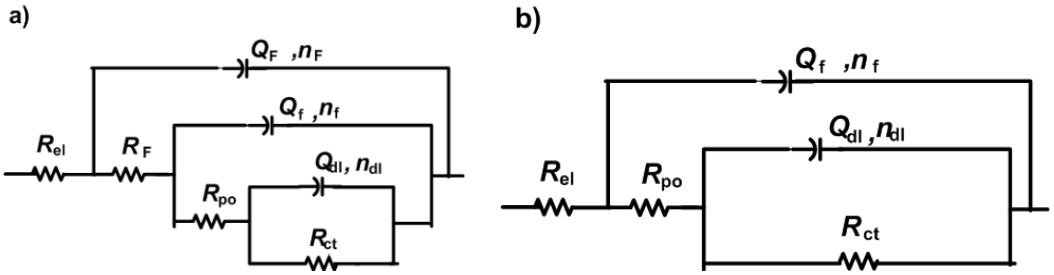


***Figure 5.*** *Electrical equivalent circuits with (a) three time constants and (b) two time constants for analysis of EIS data ($R_{el}$ - electrolyte resistance; $R_F$ - faradaic resistance of electrochemical reaction involving corrosion products; $Q_F$ - capacitance of corrosion products; $R_{po}$-resistance of pores in the coating; $Q_f$ - constant phase element representing the coating capacitance; $R_{ct}$ - charge transfer resistance; $Q_{dl}$ - constant phase element describing the double layer capacitance; $n_F$, $n_f$ and $n_{dl}$ - coefficients describing the nonideal capacitive behaviour)*

***Table 3.*** *EIS parameters for one layer of coating dried at 24°C*

| | $R_F$ / kΩ cm² | $Q_F$ / μS sⁿ cm⁻² | $n_F$ | $R_{po}$ / kΩ cm² | $Q_f$/ μS sⁿ cm⁻² | $n_f$ | $R_{ct}$ / kΩ cm² | $Q_{dl}$ / μS sⁿ cm⁻² | $n_{dl}$ |
|---|---|---|---|---|---|---|---|---|---|
| 1st day | 0.56 | 0.001 | 0.99 | 10.06 | 0.04 | 0.87 | 600 | 9.30 | 0.47 |
| 2nd day | 0.72 | 0.03 | 0.73 | 26.04 | 0.35 | 0.74 | 849 | 7.20 | 0.65 |
| 29th day | 1.12 | 0.01 | 0.79 | 65.78 | 0.14 | 0.77 | 1770 | 3.22 | 0.70 |

The EIS spectra for the coated bronze, dried at elevated temperature (55 °C), are presented in Figure 6. On the first day of exposure, the phase angle plot exhibited a wide maximum at high and medium frequency range, which is typical of a well-protecting organic coating [20,21,28,29]. During the exposure to acid rain solution, the additional peak becomes visible in the lower frequencies region, indicating the occurrence of the corrosion of metal substrate caused by the penetration of water into the coating. These changes are accompanied by a decrease in impedance modulus values. For the analysis of EIS spectra for the first and the second day of exposure, an electrical equivalent circuit with two *R*-*Q* couples was required, where the first couple describes properties of the coating, while the second one describes the corrosion reaction on the metal surface (Figure 5b) [20-22,30,31]. The obtained EIS parameters are shown in Table 4. The decrease in coating protective properties can be observed from the decrease in $R_{po}$ values. In addition, the decrease in $R_{ct}$ and the increase in $Q_{dl}$ values indicate the corrosion process on the metal substrate. Finally, an additional *R*-*Q* couple was required on the 29$^{th}$ day to describe the high-frequency region in EIS spectrum. As in the case of the previous sample, this was ascribed to the appearance of corrosion products. Interestingly, $Q_f$ value didn't change in time despite the decrease in $R_{po}$ values. This can be related to the appearance of surface blistering, which can be clearly observed on studied samples (Figure 4b). As blistering and swelling of the coating caused an increase in coating thickness, its capacitance wasn't changed much despite the entrance of the water. Considering this, it was possible that the selected drying temperature was too high, causing the cracking of the coating, which enabled the penetration of electrolyte and the formation of blisters.

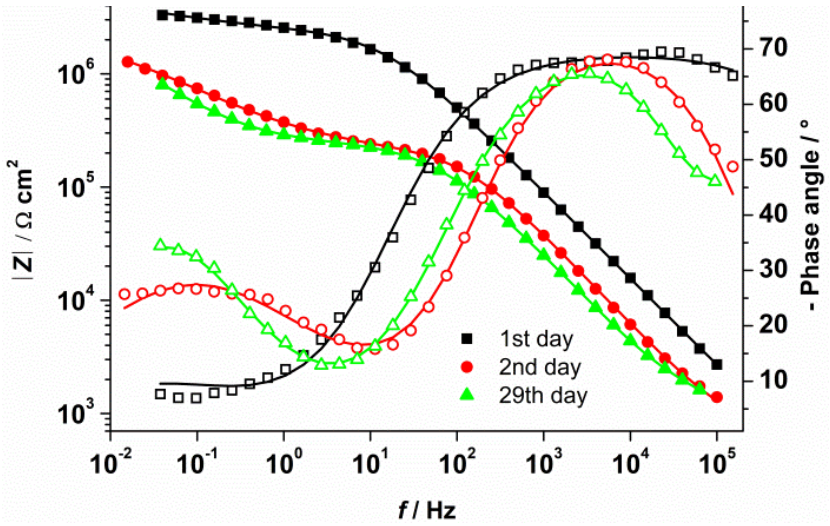


***Figure 6.*** *EIS spectra for one layer of coating dried at 55°C (solid symbols-impedance; open symbols-phase angle). Experimental data are depicted in symbols and fitted data in lines*

***Table 4.*** *EIS parameters for one layer of coating dried at 55°C*

| | $R_F$ / kΩ cm$^{-2}$ | $Q_F$ / μS s$^n$ cm$^{-2}$ | $n_F$ | $R_{po}$ / kΩ cm$^{-2}$ | $Q_f$/ μS s$^n$ cm$^{-2}$ | $n_f$ | $R_{ct}$ / kΩ cm$^{-2}$ | $Q_{dl}$ / μS s$^n$ cm$^{-2}$ | $n_{dl}$ |
|---|---|---|---|---|---|---|---|---|---|
| 1$^{st}$ day | - | - | - | 2485 | 0.01 | 0.77 | 2634 | 1.26 | 0.52 |
| 2$^{nd}$ day | - | - | - | 217.7 | 0.02 | 0.81 | 2408 | 1.92 | 0.52 |
| 29$^{th}$ day | 3.21 | 0.05 | 0.70 | 248.2 | 0.01 | 0.89 | 2200 | 3.40 | 0.68 |

The results above show that the ambient temperature was too low for coating drying and led to modest protective properties while drying at 55 °C. This resulted in excellent initial properties, but they deteriorated during exposure to an acid rain solution. For this reason, additional studies were performed with the coating dried at 40 °C. The EIS spectra of such samples are shown in Figure 7. In the Bode diagram, it can be seen that the impedance modulus values are lower than for the sample

dried at 55 °C. They decreased significantly from the first to the second day and then increased again by the end of the exposure. For the first and second days of exposure, two-phase angle maxima are clearly visible at high and low frequencies, which required an equivalent electrical circuit with two-time constants for analysis (Figure 5b). As for the previous samples, the presence of two time constants is a clear indication of the occurrence of the corrosion process on the metal surface. The data obtained from the EIS fitting are presented in Table 5. The decrease in $R_{ct}$ and the increase in $Q_{dl}$ values in time also indicate the corrosion process at the bottom of the coating, *i.e.,* on the bronze surface, caused by water penetration. The increase in $Q_f$ is also ascribed to water ingress into the coating. For the analysis of EIS spectrum collected on 29$^{th}$ day of exposure, an additional time constant was needed, pointing to the accumulation of corrosion products. The formation of corrosion products led to an increase in $R_{ct}$ value. Unlike for the sample dried at 24 °C, in this case, the presence of corrosion products was clearly observed on the metal surface, but there were no traces of coating blistering, as seen at 55 °C (Figure 4c).

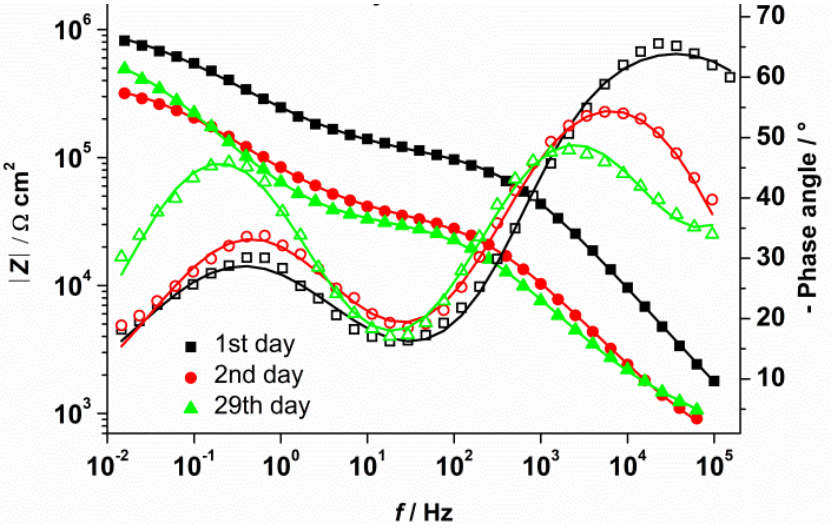


***Figure 7.*** *EIS spectra for one layer of coating dried at 40°C (solid symbols-impedance; open symbols-phase angle). Experimental data are depicted in symbols and fitted data in lines*

***Table 5.*** *EIS parameters for one layer of coating dried at 40°C*

| | $R_F$ / kΩ cm$^{-2}$ | $Q_F$ / μS s$^n$ cm$^{-2}$ | $n_F$ | $R_{po}$ / kΩ cm$^{-2}$ | $Q_f$/ μS s$^n$ cm$^{-2}$ | $n_f$ | $R_{ct}$ / kΩ cm$^{-2}$ | $Q_{dl}$/ μS s$^n$ cm$^{-2}$ | $n_{dl}$ |
|---|---|---|---|---|---|---|---|---|---|
| 1$^{st}$ day | - | - | - | 107 | 0.02 | 0.76 | 1090 | 2.00 | 0.55 |
| 2$^{nd}$ day | - | - | - | 34.75 | 0.14 | 0.73 | 384 | 5.01 | 0.61 |
| 29$^{th}$ day | 1.45 | 0.04 | 0.71 | 30.89 | 0.18 | 0.73 | 728 | 5.75 | 0.72 |

Additionally, the influence of coating application in three layers (of total thickness not higher than one layer coating) was examined. Each additional layer was applied after 24 hours and cured at 40 °C for 4 hours. The obtained EIS spectra are presented in Figure 8. The Bode plot showed an increase in impedance modulus values, which was more pronounced at the beginning of the exposure. In the phase angle plots, again for the first two days, two maxima were observed that required the electrical equivalent circuit presented in Figure 5b for fitting. A circuit with three time constants (Figure 5a) was needed for the 29$^{th}$ day of exposure. The data obtained by fitting are shown in Table 6. Similarly to previous samples, an increase in $Q_f$ value is observed on the second day of immersion, which is attributed to the water ingress into the coating. However, $R_{po}$ and $R_{ct}$ values increased at the same time, followed by a decrease in $Q_{dl}$. This could be attributed to the formation of corrosion products, but they were not observed on the metal surface (Figure 9) nor could be deduced from the impedance spectra.

Similar results were also obtained in our previous study on this coating [32]. The increase in $R_{po}$ can be attributed to the swelling of the polymer particles due to water uptake into the coating and closure of the pores as the result of this process, as was concluded from the study of Lendvay-Gyorik *et al.* [33], as well in the study of Ecco *et al.* [34]. Similarly, Le Pen *et al*. [35] observed an increase in pore resistance of waterborne coating during the first days of immersion, which was attributed to the coalescence process. Such conclusions are also in agreement with an increase in $R_{ct}$ values and lower $Q_{dl}$ values for the second day of immersion. However, on the last day of immersion, an additional phase angle maximum in the high-frequency region is observed, corresponding to the presence of corrosion products. As the water was present in the coating and at the metal/coating interface, it is not surprising that, with time, some corrosion products accumulated on the surface and in the pores of the coating. However, they could not be seen by the bare eye (Figure 9) as for one layer coating.

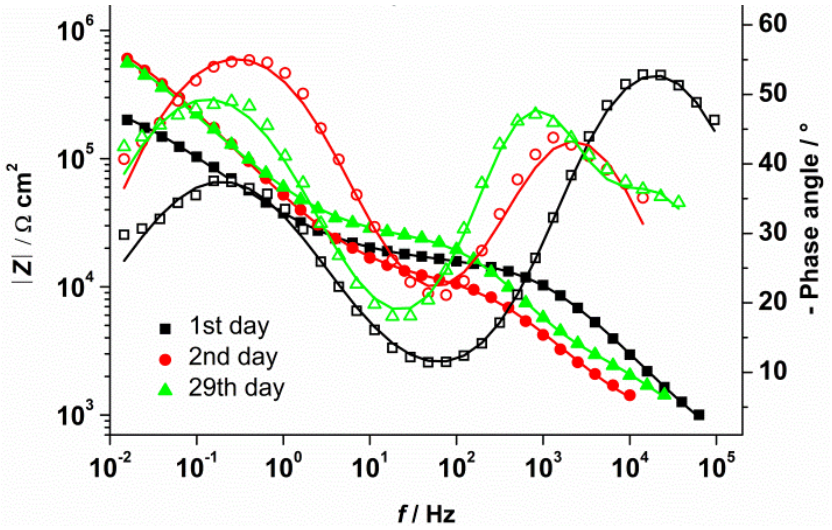


***Figure 8.*** *EIS spectra for three layers of coating dried at 40°C (solid symbols-impedance; open symbols-phase angle). Experimental data are depicted in symbols and fitted data in lines*

***Table 6.*** *EIS parameters for three layers of coating dried at 40°C*

| | $R_F$ / kΩ cm$^2$ | $Q_F$ / μS s$^n$ cm$^{-2}$ | $n_F$ | $R_{po}$ / kΩ cm$^2$ | $Q_f$/ μS s$^n$ cm$^{-2}$ | $n_f$ | $R_{ct}$ / kΩ cm$^2$ | $Q_{dl}$ / μS s$^n$ cm$^{-2}$ | $n_{dl}$ |
|---|---|---|---|---|---|---|---|---|---|
| 1$^{st}$ day | - | - | - | 15.8 | 0.08 | 0.75 | 351.8 | 12.1 | 0.61 |
| 2$^{nd}$ day | - | - | - | 11.9 | 0.32 | 0.75 | 1200 | 5.43 | 0.72 |
| 29$^{th}$ day | 3.39 | 0.05 | 0.83 | 21.1 | 0.07 | 0.88 | 1350 | 6.20 | 0.68 |

***Figure 9****. Surface image of three layers of waterborne acrylic coating C1 coated on a RG7 bronze where each layer was dried at 40 °C for 4 hours*

From these results, it can be concluded that better protective properties are obtained if the coating is applied in three thinner layers than in one thicker layer, which can probably be ascribed to more efficient drying in the first case. In addition, the observed improvement of protective properties of the

three-layer coating during the sample immersion in acid rain solution was probably due to the coating swelling, while in the case of one-layer coating, the formation of corrosion products was a dominant phenomenon, visible by the naked eye, which can be related to coating cracking during the drying process.

Supplementary studies were conducted on bronze samples protected by coating C2, which is also an acrylic waterborne coating but with slightly higher water content and without a corrosion inhibitor that could reduce the corrosion rate of the metal substrate. Figure 10 presents the EIS spectrum for RG7 bronze protected with C2, applied in three layers and dried at 40 °C.

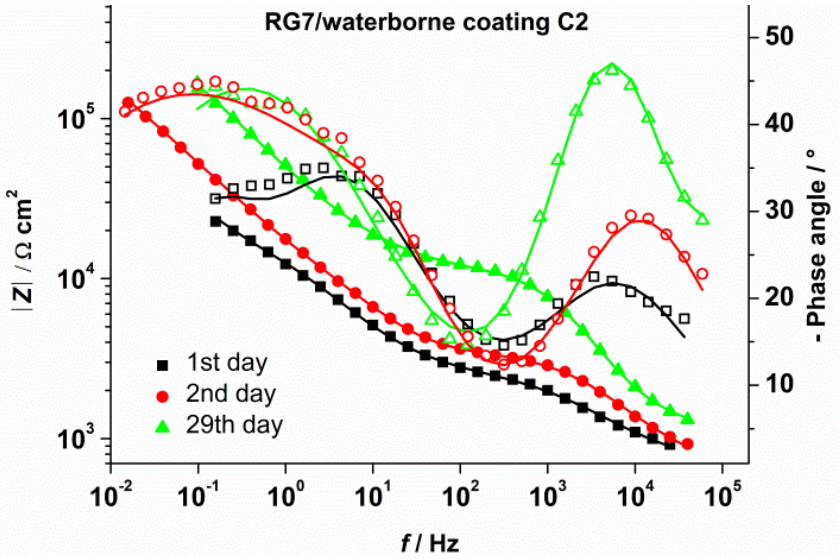


***Figure 10.*** *EIS spectra for three layers of coating C2 dried at 40°C (solid symbols-impedance; open symbols-phase angle). Experimental data are depicted in symbols and fitted data in lines*

It can be observed that impedance modulus values increased in time, in a whole frequency range, which means that the corrosion resistance increases with the immersion time. Still, C2 coating showed lower protective properties compared to C1 coating. It is also interesting to note that the impedance modulus values, both at high and low frequencies, increased with the immersion time, indicating improved coating barrier properties. For these spectra, it was necessary to use an electrical equivalent circuit with three *R*-*Q* pairs in order to achieve satisfactory fitting quality. It is similar to the one presented in Figure 5a, but the $R_F$-$Q_F$ couple is related to the medium-frequency region, as in these spectra, two phase angle maxima are observed in the medium and low-frequency regions. The EIS parameters obtained by fitting are listed in Table 7.

***Table 7.*** *EIS parameters for three layers of coating C2 dried at 40°C*

| | $R_{po}$ / kΩ cm² | $Q_f$ / μS sⁿ cm⁻² | $n_f$ | $R_F$ / kΩ cm² | $Q_F$/ μS sⁿ cm⁻² | $n_F$ | $R_{ct}$ / kΩ cm² | $Q_{dl}$ / μS sⁿ cm⁻² | $n_{dl}$ |
|---|---|---|---|---|---|---|---|---|---|
| 1st day | 2.04 | 1.18 | 0.66 | 19.7 | 15.9 | 0.69 | 33.0 | 51.3 | 0.83 |
| 2nd day | 2.93 | 0.32 | 0.72 | 6.55 | 4.60 | 0.87 | 803 | 22.8 | 0.54 |
| 29th day | 1.45 | 0.004 | 0.87 | 9.65 | 0.03 | 0.90 | 695 | 7.35 | 0.61 |

In general, for C2 coating, a greater decrease in capacitance values at all frequencies is observed, probably as a result of the swelling of the coating and closure of the pores, which also contributed to the $R_{ct}$ increase. This time, $R_{ct}$ values are significantly lower than for the previously tested C1 coating. This increase in resistance, once again, could be ascribed to the formation of corrosion products. Their presence here is not noticeable as one layer of C1 dried at 40 °C, but this time coating

turned bluish, indicating the presence of copper ions. The assumption is that the copper ions probably slowly came out through the coating during immersion in acid rain solution.

Further study includes gravimetric measurements, which were carried out with the aim to analyse water absorption by coating. Gravimetric measurements of both tested coatings showed the same trend, presented in Table 8. After 8 h of immersion in acid rain solution, an increase in mass could be observed, which is explained by the fact that the coating took up a certain amount of water. This phenomenon is found in the case of physically drying resins and paints. There are still many pores in the dry film through which water can penetrate, resulting in coating swelling [33]. However, after 5 days of immersion, mass loss was noticed. Although dry coating cannot be dissolved anymore, it is possible that water could still dissolve certain components and polymer particles of low-degree polymerization [33]. Roggero *et al*. [36] associated this mass loss with the release of plasticizer from the formulation. They noted possible leaching or release of soluble coating components due to water penetration into the coating. When comparing the two studied coatings, greater water absorption and consequent mass loss were obtained for C2 coating, which already contained a larger amount of water in its composition compared to C1.

***Table 8.*** *Results of gravimetric analysis for coatings dried at 40 °C samples and immersed in acid rain solution*

| Sample | Mass before immersion, g | Mass change after 8 h of immersion, % | Mass change after 126 h of immersion, % |
|---|---|---|---|
| C1 | 0.312 | + 30 | + 9 |
| C2 | 0.361 | + 41 | + 29 |

*Comparison between two waterborne coatings on different bronze substrates*

Previous results have shown that incomplete coating drying can lead to substrate corrosion. Therefore, substrate corrosion resistance could be important for overall coating performance. For this reason, corrosion protection by C1 and C2 was examined on different bronze substrates. Linear polarization measurements were conducted to evaluate polarization resistance values during three weeks of immersion in artificial acid rain solution (Figure 11).

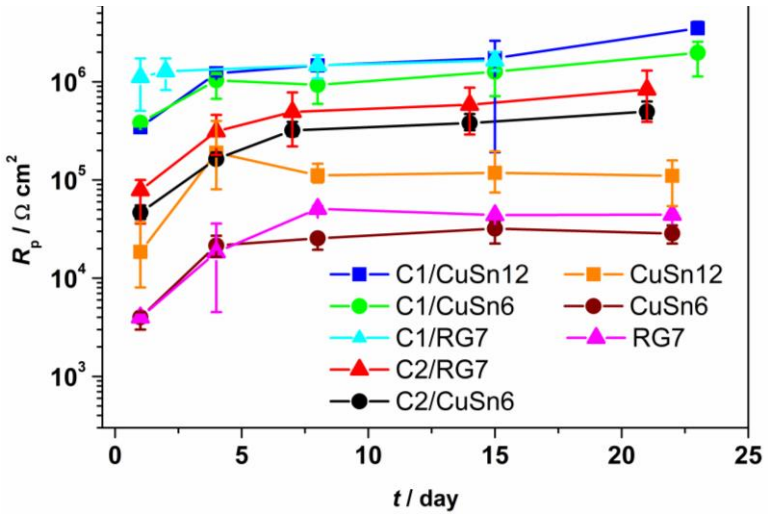


***Figure 11.*** *Dependence of polarization resistance on time for two waterborne coatings on different bronze substrates*

It can be seen that the $R_p$ values were higher for all bronzes protected with C1 than when protected with C2, although both provided corrosion protection to bronze surfaces. Another thing to emphasize is the trend of constant growth of resistance for all coated samples. This trend can be related to the coating swelling (expected in the first days of immersion) [35,18], although some

increase due to the plugging of the pores by corrosion products cannot be neglected. In principle, the higher the corrosion resistance of the bronze substrate alone, the higher the corrosion resistance of the coated sample. For all examined bronzes, significant corrosion protection can be achieved by both studied waterborne coatings, especially by C1 coating.

*Waterborne coatings on patinated bronze substrates*

As mentioned in the Introduction section, bronze exposed to a corrosive environment gradually covers with corrosion products called patina. Its composition depends on the concentration and type of present aggressive ions. Patina is also often formed artificially in order to achieve the aesthetically pleasant appearance of bronze sculptures. In this work, two types of bronze patina are used, chemically formed dark brown patina as a common type of artificial patina on bronze [37] and electrochemically formed green-bluish patina representing aged patina, consisting of copper sulphates or carbonates [3,38,39]. In this work, the protection of patinated substrates by waterborne coating C1 was investigated. Since the lower drying temperature resulted in the formation of small bubbles in the coating and a modest level of corrosion protection for bare bronze, while at higher temperature exposure to the corrosive medium resulted in coating blistering, the drying temperature for the protective coating of already reactive artificial patina substrates was 40 °C. The coating application was performed in three layers due to more efficient drying.

Studies were conducted using polarization resistance measurements during three weeks of exposure to an artificial acid rain solution (Figure 12). It can be observed that for all patinated bronzes, C1 coating provided a high level of corrosion protection. In the case of coated sulphide patina, the $R_p$ values were the highest for CuSn12 bronze. Similarly to the case of bare bronze substrates, the trend of constant growth of resistance attributed to coating swelling was present [35,18]. Such a trend was also observed for electrochemical patina on two different bronze substrates protected with waterborne coating, only this time, the resistance was higher for CuSn6 bronze.

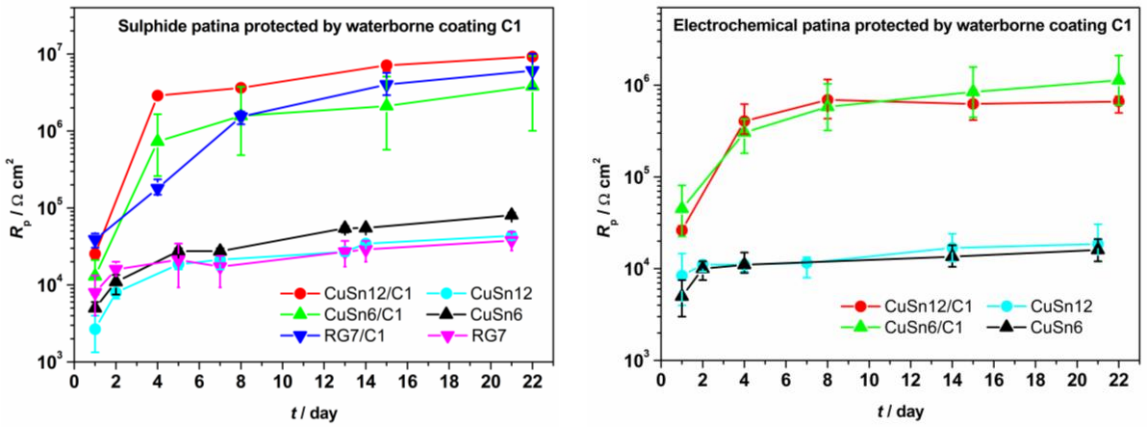


***Figure 12.*** *Polarization resistance on time for waterborne coating C1 on differently patinated bronze substrates. (a) Sulphide and (b) electrochemical patina formed on various types of bronze*

Another important thing to emphasize is that the selected waterborne coating does not alter the visual appearance of the patinas, as shown in Figure 13. There was no change of colour of the patina upon the coating application, as well as during the exposure to acid rain [18]. This confirms the suitability of C1 coating for application on patinated bronze as it enhances the stability of the patina layer.

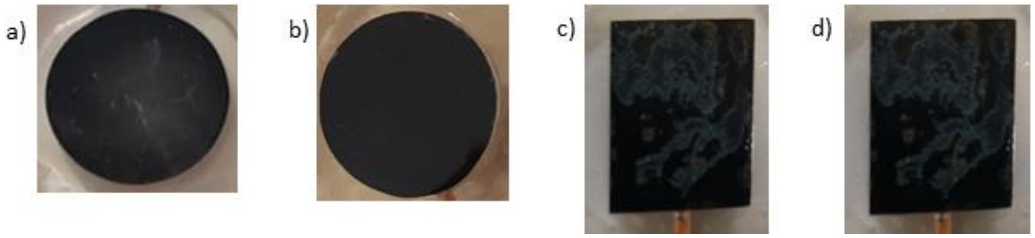


***Figure 13**. Visual appearance of bronze sample with (a) sulphide patina, (b) sulphide patina with C1, (c) electrochemical patina and (d) electrochemical patina with C1 before exposure*

## Conclusions

The investigation of the influence of drying temperature on acrylic waterborne coating protective properties showed that the temperature had a significant impact on coating performance. It was found that drying at ambient temperature resulted in the formation of small bubbles in dry coating and modest corrosion protection. Although the sample polarization resistance values increased during the three-week immersion in artificial rain solution, from EIS spectra, it appeared that this was the consequence of the formation of corrosion products that were plugging the pores of the coating. Drying at 55 °C resulted in greater initial corrosion protection, but the degradation occurred during exposure to acid rain solution. Moreover, the coating blistering was observed. The one-layer coating dried at 40 °C showed inadequate protection stability as the formation of corrosion products was observed, however, when the coating was applied in three layers, there were no visible corrosion products. In addition, the resistance values increased for the whole exposure time, which was attributed to swelling of the polymer particles due to water uptake into the coating and closure of the pores.

The level of protection between two acrylic coatings that differ in the amount of water and the presence of corrosion inhibitor was compared. The coating with a lower amount of water and corrosion inhibitor exhibited better protective properties for different bronze substrates. In general, the higher the corrosion resistance of bare bronze, the better the performance of the coating.

This study also revealed that coating C1 is suitable for the protection of artificially patinated bronzes as the patina layer surface is not changed by coating application and remains stable in time.

***Acknowledgements**: This work was fully supported and funded by the Croatian Science Foundation under the project IP-2019-04-5030.*

***Conflicts of interest**: The authors declare to have no competing financial interest or personal relation that could influence the results of this work.*

## References

[1] M. Wadsak, I. Constantinides, G. Vittiglio, A. Adriaens, K. Janssens, M. Schreiner, F.C. Adams, P. Brunella, M. Wuttmann, Multianalytical study of patina formed on archaeological metal objects from Bliesbruck-Reinheim, *Microchimica Acta* **133** (2000) 159–164. https://doi.org/10.1007/s006040070086

[2] D.A. Scott, *Copper and Bronze in Art: Corrosion, colorants, conservation*, Getty Publications, Los Angeles, California, 2002, p. 277.

[3] G. Di Carlo, C. Giuliani, C. Riccucci, M. Pascucci, E. Mesina, G. Fierro, M. Lavorgna, G.M. Ingo, Artificial patina formation onto copper-based alloys: chloride and sulphate induced corrosion processes, *Applied Surface Science* **421** (2017) 120-127. https://doi.org/10.1016/j.apsusc.2017.01.080

[4] E. Rocca, F. Mirambet, in *Corrosion of metallic heritage artefacts, investigation, conservation and prediction for long-term behavior*, P. Dillmann, G. Beranger, P. Piccardo, H. Matthiesen, Woodhead Publishing, City, USA, 2007, p. 308-334.
[5] J. Hu, K. Peng, J. Guo, D. Shan, G.B. Kim, Q. Li, E. Gerhard, L. Zhu, W. Tu, W. Lv, M.A. Hickner, J. Yang, Click crosslinking improved waterborne polymers for environment-friendly coatings and adhesives, *Applied Materials and Interfaces* **8** (2016) 17499–17510. https://doi.org/10.1021/acsami.6b02131
[6] R. Hischier, B. Nowack, F. Gottschalk, I. Hincapie, M. Steinfeldt, C. Som, Life cycle assessment of façade coating systems containing manufactured nanomaterials, *Journal of Nanoparticle Research* **17** (2015) 68. https://doi.org/10.1007/s11051-015-2881-0
[7] J.L. Hall, A. Pérez, E.L. Kynaston, C. Lindsay, J.L. Keddie, Effects of environmental conditions on the micro-mechanical properties of formulate waterborne coatings, *Progress in Organic Coatings* **163** (2022) 106657. https://doi.org/10.1016/j.porgcoat.2021.106657
[8] E. Almeida, D. Santos, J. Uruchurtu, Corrosion performance of waterborne coatings for structural steel, *Progress in Organic Coatings* **37** (1999) 131-140. https://doi.org/10.1016/S0300-9440(99)00064-8
[9] V. Duecoffre, W. Diener, C. Flosbach, W. Schubert, Emulsifiers with high chemical resistance: a key to high performance waterborne coatings, *Progress in Organic Coatings* **34** (1998) 200-205. https://doi.org/10.1016/S0300-9440(98)00032-0
[10] F. Galliano, D. Landolt, Evaluation of corrosion protection properties of additives for waterborne epoxy coatings on steel, *Progress in Organic Coatings* **44** (2002) 217-225. https://doi.org/10.1016/S0300-9440(02)00016-4
[11] T.D. Martins, M.T. Viciosa, M.B. Oliveira, A. Fernandes, J.F. Mano, C. Baleizão, J.P.S. Farinha, Reversible imine crosslinking in waterborne self-healing polymer coatings, *Progress in Organic Coatings* **180** (2023) 107552. https://doi.org/10.1016/j.porgcoat.2023.107552
[12] M.E. Belowich, J.F. Stoddart, Dynamic imine chemistry, *Chemical Society Reviews* **41** (2012) 2003-2004. https://doi.org/10.1039/c2cs15305j
[13] J.M.G. Martinho, J.P.S. Farinha, Analytical series: fluorescence decay methods for the characterization of latex film formation, *Journal of Coatings Technology and Research* **10** (2013) 42-49.
[14] S. Piçarra, C.A.M. Afonso, V.B. Kurteva, A. Fedorov, J.M.G. Martinho, J.P.S. Farinha, The influence of nanoparticle architecture on latex film formation and healing properties, *Journal of Colloid and Interface Science* **368** (2012) 21-33. https://doi.org/10.1016/j.jcis.2011.10.077
[15] A. Aradian, E. Raphaël, P.G. de Gennes, Strengthening of a polymer interface: interdiffusion and cross-linking, *Macromolecules* **33** (2000) 9444-9451. https://doi.org/10.1021/ma0010581
[16] I. Stojanović, I. Juraga, V. Alar, Influence of drying temperature on protective properties of waterborne and solventborne epoxy coating, *International Journal of Electrochemical Science* **9** (2014) 2507-2517. https://doi.org/10.1016/S1452-3981(23)07943-9
[17] H.-D. Hwang, J.-I. Moon, J.H. Choi, H.-J. Kim, S.D. Kim, J.C. Park, Effect of water drying conditions on the surface property and morphology of waterborne UV-curable coatings for engineered flooring, *Journal of Industrial and Engineering Chemistry* **158** (2009) 381-387. https://doi.org/10.1016/j.jiec.2008.11.002
[18] A. Kapitanović, H. Otmačić Ćurković, The influence of phosphonic acid pretreatment on the bronze corrosion protection by waterborne coating, *Journal of Solid State Electrochemistry* **27** (2023) 1861-1875. https://doi.org/10.1007/s10008-023-05490-1

[19] T. Kosec, A. Legat, I. Milošev, The comparison of organic protective layers on bronze and copper, *Progress in Organic Coatings* **69** (2010) 199-206. https://doi.org/10.1016/j.porgcoat.2010.04.010
[20] F. Mansfeld, Use of electrochemical impedance spectroscopy for the study of corrosion protection by polymer coatings, *Journal of Applied Electrochemistry* **25** (1995) 187-202. https://doi.org/10.1007/BF00262955
[21] E. Cano, D. Lafuente, D.M. Bastidas, Use of EIS for the evaluation of the protective properties of coatings for metallic cultural heritage: a review, *Journal of Solid State Electrochemistry* **14** (2010) 381-391. https://doi.org/10.1007/s10008-009-0902-6
[22] E. Cano, D.M. Bastidas, V. Argyropoulos, S. Fajardo, A. Siatou, J.M. Bastidas, C. Degrigny, Electrochemical characterization of organic coatings for protection of historic steel artefacts, *Journal of Solid State Electrochemistry* **14** (2010) 453-463. https://doi.org/10.1007/s10008-009-0907-1
[23] H. Wang, P. Zhang, G. Fei, Y. Ma, N. Rang, Y. Kang, Design and properties of environmental anticorrosion coating based on *m*-aminobenzenesulfonic acid/aniline/*p*-phenylenediamine terpolymer, *Progress in Organic Coatings* **137** (2019) 105274. https://doi.org/10.1016/j.porgcoat.2019.105274
[24] L. Jianguo, G. Gaoping, Y. Chuanwei, EIS study of corrosion behaviour of organic coating/Dacromet composite systems, *Electrochimica Acta* **50** (2005) 3320-3332. https://doi.org/10.1016/j.electacta.2004.12.010
[25] A. Collazo, B. Díaz, R. Figueroa, X.R. Nóvoa, C. Pérez, Corrosion resistance of a water-borne resin doped with graphene derivatives applied on galvanized steel, *Progress in Organic Coatings* **173** (2022) 107220. https://doi.org/10.1016/j.porgcoat.2022.107220
[26] A. Miszczyk, K. Darowicki, Water uptake in protective organic coatings and its reflection in measured coating impedance, *Progress in Organic Coatings* **124** (2018) 296-302. https://doi.org/10.1016/j.porgcoat.2018.03.002
[27] F. Bellucci, L. Nicodemo, Water transport in organic coatings, *Corrosion* **49** (1993) 235-247. https://doi.org/10.5006/1.3316044
[28] G. Grundmeier, W. Schmidt, M. Stratmann, Corrosion protection by organic coatings: electrochemical mechanism and novel methods of investigation, *Electrochimica Acta* **45** (2000) 2515-2533. https://doi.org/10.1016/S0013-4686(00)00348-0
[29] H. Qian, X. Fu, Y. Chi, R. Zhang, C. Zhan, H. Sun, X. Zhou, J. Sun, Study on electrodeposition and corrosion resistance of Cu-Sn alloy prepared in ChCl-EG deep eutectic solvent, *Journal of Solid State Electrochemistry* **26** (2002) 469-479. https://doi.org/10.1007/s10008-021-05086-7
[30] B. Dou, H. Xiao X. Lin, Y. Zhang, S. Zhao, S. Duan, X. Gao, Z. Fang, Investigation of the anti-corrosion properties of fluorinated graphene-modified waterborne epoxy coatings for carbon steel, *Coatings* **11** (2021) 254. https://doi.org/10.3390/coatings11020254
[31] J.B. Bajat, I. Milošev, Ž. Jovanović, V.B. Mišković-Stanković, Studies on adhesion characteristics and corrosion behaviour of vinyltriethoxysilane/epoxy coating protective system on aluminium, *Applied Surface Science* **256** (2010) 3508-3517. https://doi.org/10.1016/j.apsusc.2009.12.100
[32] A. Kapitanović, T. Kokot, H. Otmačić Ćurković, Bronze corrosion protection by bilayer systems: self-assembled monolayers of phosphonic acid/waterborne acrylic coating, *Progress in Organic Coatings* **186** (2024) 107984. https://doi.org/10.1016/j.porgcoat.2023.107984
[33] G. Lendvay-Györik, T. Pajkossy, B. Lengyel, Corrosion-protection properties of water-borne paint coatings as studied by electrochemical impedance spectroscopy and gravimetry.

*Progress in Organic Coatings* **56** (2006) 304-310. https://doi.org/10.1016/j.porgcoat.2006.05.012

[34] L.G. Ecco, J. Li, M. Fedel, F. Deflorian, J. Pan, EIS and in situ AFM study of barrier property and stability of waterborne and solventborne clear coats, *Progress in Organic Coatings* **77** (2014) 600-608. http://dx.doi.org/10.1016/j.porgcoat.2013.11.024

[35] C. Le Pen, C. Lacabanne, N. Pébère, Characterisation of water-based coatings by electrochemical impedance spectroscopy, *Progress in Organic Coatings* **46** (2003) 77-83. https://doi.org/10.1016/S0300-9440(02)00213-8

[36] A. Roggero, L. Villareal, N. Caussé, A. Santos, N. Pébère, Correlation between the physical structure of a commercially formulated epoxy paint and its electrochemical impedance response, *Progress in Organic Coatings* **146** (2020) 105729. https://doi.org//10.1016/j.porgcoat.2020.105729

[37] A. Kapitanović, H. Otmačić Ćurković, The effect of corrosion conditions on aging of artificial patina on three bronzes, *Coatings* **12** (2022) 936. https://doi.org/10.3390/coatings12070936

[38] K. Marušić, H. Otmačić-Ćurković, Š. Horvat-Kurbegović, H. Takenouti, E. Stupnišek-Lisac, Comparative studies of chemical and alectrochemical preparation of artificial bronze patinas and their protection by corrosion inhibitor, *Electrochimica Acta* **54** (2009) 7106-7113. https://doi.org/10.1016/j.electacta.2009.07.014

[39] G. Masi, J. Esvan, C. Josse, C. Chiavari, E. Bernardi, C. Martini, M.C. Bignozzi, N. Gartner, T. Kosec, L. Robbiola, Characterisation of typical patinas simulating bronze corrosion in outdoor conditions, *Material Chemistry and Physics* **200** (2017) 308-321. https://doi.org/10.1016/j.matchemphys.2017.07.091